Electronic Supplementary Material (ESI) for Materials Horizons.

Supporting Information for:

Tunable internal quantum well alignment in rationally designed oligomer-based perovskite films deposited by resonant infrared matrix-assisted pulsed laser evaporation

Wiley A. Dunlap-Shohl,[a] E. Tomas Barraza,[b] Andrew Barrette,[c] Seyitliyev Dovletgeldi,[c] Gamze Findik,[c] David J. Dirkes,[d] Chi Liu,[e] Manoj K. Jana,[a,e] Volker Blum, [a,e] Wei You,[d] Kenan Gundogdu,[c] Adrienne D. Stiff-Roberts,[b] David B. Mitzi [a,e]

[a]Department of Mechanical Engineering and Materials Science, Duke University, Durham, North Carolina 27708, United States

[b]Department of Electrical and Computer Engineering, Duke University, Durham, North Carolina 27708, United States

[c]Department of Physics, North Carolina State University, Raleigh, North Carolina 27695, United States

[d]Department of Chemistry, University of North Carolina at Chapel Hill, Chapel Hill, North Carolina 27599, United States

[e]Department of Chemistry, Duke University, Durham, North Carolina 27708, United States

Synthesis of AE2T·2HI and AE4T·2HX Salts.

AE2T·2HI Synthesis (see Scheme 1a in the main article):

tert-butyl (2-(thiophen-2-yl)ethyl)carbamate (1)

6.89 g (54.14 mmol, 1.0 eq) thiophene-2-ethylamine was weighed out and added to a flame dried 500 mL round-bottom flask (RBF) under inert atmosphere, followed by 11.7 mL (8.49 g, 83.9 mmol, 1.55 eq) of freshly distilled, dry triethylamine added by syringe. 130 mL of dry DCM was then added to the reaction flask by cannula under inert atmosphere and the mixture was stirred. In a separate flame-dried 100 mL RBF, 14.2 g (65.0 mmol, 1.2 eq) of di-tert-butyl dicarbonate (Boc_2O) was quickly weighed out, put under inert atmosphere, and then dissolved in 30 mL of dry DCM. The Boc_2O solution was taken up in a syringe and slowly added to the stirring thiophene-2-ethylamine solution dropwise. The reaction mixture was left to stir and react for three days. The crude reaction mixture (RM) was diluted with 150 mL DCM, poured into 200 mL of water in a 1 L separator funnel, and washed with water three times (3 × 200 mL). Additional product was recovered from the combined aqueous layers by extracting with fresh DCM (3 × 100 mL). The combined DCM layers were dried with magnesium sulfate, vacuum filtered, and concentrated, providing the crude product as a clear oil. Further purification by vacuum distillation in a 100 °C oil bath under high vacuum (0.3 torr) provided residual starting material in the first distillation fraction and the desired product in the second fraction as a clear oil. The ^1H nuclear magnetic resonance (NMR) spectrum of **1** is given in Figure S7.

Yield: 12.1 g (98% yield)

^1H NMR (600 MHz, Chloroform-*d*) δ 7.16 (dd, *J* = 5.1, 1.1 Hz, 1H), 6.94 (dd, *J* = 5.1, 3.4 Hz, 1H), 6.85 – 6.81 (m, 1H), 4.67 (s, 1H, N-H), 3.44 – 3.37 (m, 2H), 3.02 (t, *J* = 6.6 Hz, 2H), 1.44 (s, 9H).

tert-butyl (2-(5-bromothiophen-2-yl)ethyl)carbamate (2)

6.279 g (27.62 mmol, 1.0 eq) of compound **1** was weighed out into a 250 mL RBF and then dissolved in 85 mL of DMF. The flask was covered with tin foil to shield the solution from light, put under an inert atmosphere, and the mixture was cooled to 0 °C in an ice water bath. In a separate 100 mL tin foil covered RBF, 4.698 g (26.39 mmol, 0.955 eq) of solid *n*-bromosuccinimide (NBS) was dissolved in 40 mL of DMF in the dark under an inert atmosphere, while cooled to 0°C in an ice water bath. These two flasks were stirred at 0°C for 30 minutes. Using a 50 mL syringe, the NBS solution was added to the 0°C flask containing compound **1** dropwise under minimal light. The RM was left to stir and slowly warm back to room temperature (RT) in the dark overnight. The next morning, the RM was taken up in diethyl ether, poured into a 1 L separator funnel, washed with water (500 mL), and extracted three times with diethyl-ether (3 × 150 mL). The diethyl ether layer was dried with magnesium sulfate, vacuum filtered, and concentrated via rotary evaporation. Residual DMF was removed from the concentrated product using high vacuum over 48 hrs, and the product was obtained as a clear oil. The product was fully brominated by ^{1}H NMR and sufficiently pure to use without further purification. The ^{1}H nuclear magnetic resonance (NMR) spectrum of **2** is given in Figure S8.

Yield: 8.6 g with minimal residual DMF (quantitative yield)

^{1}H NMR (600 MHz, Chloroform-*d*) δ 6.87 (d, J = 3.6 Hz, 1H), 6.58 (d, J = 3.6 Hz, 1H), 4.69 (s, 1H, N-H), 3.40 – 3.25 (m, 2H), 2.93 – 2.89 (m, 2H), 1.43 (s, 9H).

tert-butyl (2-(5-(tributylstannyl)thiophen-2-yl)ethyl)carbamate (3)

5.51 g (24.2 mmol, 1.0 eq) of compound **1** was added to a flame dried 500 mL RBF under inert atmosphere. The flask was purged with argon for 10 minutes, and then 200 mL of dry THF was added by cannula. The mixture was cooled to 0°C in an ice water bath, and then 21.3 mL (53.2 mmol, 2.2 eq) of 2.5 M *n*-butyllithium (*n*-BuLi) in hexanes was added to the RM dropwise. (Note: while the solution remained colorless as the first equivalent of n-BuLi was added, it turned yellow, opaque, and thickened with the addition of the second equivalent. Stirring speed was increased to 800 RPM to keep the solution stirring.) After 45 minutes at 0°C, 17.72 g (14.7 mL, 54.4 mmol, 2.25 eq) of 95% tributyltinchloride was weighed out in a syringe and added to the 0°C RM dropwise. (Note: the solution changes from muddy orange to clear dark orange with the addition of the tributyltinchloride.) The RM was stirred for three days under argon. The crude RM was concentrated by rotary evaporation to remove the THF solvent, before being taken up in diethyl ether and washed three times with water (3 × 200 mL). The diethyl ether layer was dried with magnesium sulfate, vacuum filtered, and concentrated, providing the crude product as a thick black oil. Residual tin biproducts were removed from the crude product with flash chromatography, using a one inch deep silica gel plug. The product was loaded onto the plug and first washed with 1 L of hexanes, before switching to a 9:1 hexanes:ethyl acetate mixture (500 mL) to elute the product. The eluent was concentrated by rotary evaporation to provide a clear oil mixture of compound **1** (starting material) and the desired product, which was used without further purification. The ^{1}H NMR spectrum of this mixture is given in Figure S9.

Yield: 7.9 g (73% yield)

^{1}H NMR (600 MHz, Chloroform-*d*) δ 7.00 (d, *J* = 3.2 Hz, 1H), 6.95 (d, *J* = 3.2 Hz, 1H), 4.67 (s, 1H, N-H), 3.47 – 3.29 (m, 2H), 3.12 – 2.96 (m, 2H), 1.59 – 1.52 (m, 6H), 1.44 (s, 9H), 1.37 – 1.30 (m, 6H), 1.14 – 1.02 (m, 6H), 0.94 – 0.87 (t, J = 7.3 Hz, 9H).

di-tert-butyl ([2,2'-bithiophene]-5,5'-diylbis(ethane-2,1-diyl))dicarbamate (4)

To a flame dried, 3-neck 250 mL RBF with reflux condenser under inert atmosphere was added 125 mL of dry DMF. 1.50 g (4.90 mmol, 1.0 eq) compound **2** and 3.81 g (5.39 mmol, 1.1 eq) of the mixture of compounds **1** and **3** (73% by weight **3)** were weighed out in syringes and added to the reaction flask. 0.170 g (0.147 mmol, 0.03 eq) of solid tetrakis(triphenylphosphine)palladium(0) ($Pd(PPh_3)_4$) was then added to the RM and the flask was purged with argon for 10 minutes. The mixture was stirred, heated to 68°C, and left to react overnight under argon. The reaction showed complete conversion by ^{1}H NMR after 16 hrs. The RM was cooled to RT, taken up in dichloromethane, and washed with water five times (5 × 150 mL). The dichloromethane layer was dried over magnesium sulfate, vacuum filtered, and concentrated via rotary evaporation. Residual DMF was removed from the concentrated crude product using high vacuum over 48 hrs. The crude product was purified by silica column chromatography in 30:1 DCM:ethyl acetate, providing the pure product as a beige crystalline solid. The ^{1}H NMR spectrum of compound **4** is given in Figure S10.

Yield: 1.48 g (63% yield)

^{1}H NMR (400 MHz, Chloroform-*d*) δ 6.93 (d, *J* = 3.5 Hz, 2H), 6.71 (d, *J* = 3.5 Hz, 2H), 4.68 (s, 2H, N-H), 3.53 – 3.26 (m, 4H), 2.97 (t, *J* = 6.5 Hz, 4H), 1.45 (s, 18H).

5,5'-diylbis(amino-ethyl)-[2,2'-bithiophene] dihydroiodic acid salt AE2T·2HI (5-I)

0.594 g (1.31 mmol, 1.0 eq) compound **4** was weighed out and added to a 50 mL RBF covered with tin foil to shield the reaction from light, put under inert atmosphere, and dissolved in 25 mL of 1,4-dioxane. Once all of the starting material dissolved, 7 mL of freshly purified, stabilizer-free* 57% hydroiodic acid was added to the stirring reaction mixture, deprotecting the amine and quickly generating the desired ammonium-halide salt as a white precipitate. After stirring for three hours under inert atmosphere, the ammonium halide solid product was isolated from the crude RM by vacuum filtration. The filtered solid was washed with 30 mL of 1,4-dioxane and then 30 mL of $CHCl_3$. The product was collected and dried under high vacuum overnight, providing the pure product as a solid white powder. The ^{1}H NMR spectrum of compound **5-I** is given in Figure S11.

Yield: 0.489 g (73% yield)

^{1}H NMR (600 MHz, DMSO-d_6) δ 7.78 (s, 6H), 7.11 (d, *J* = 3.6 Hz, 2H), 6.93 (d, *J* = 3.6 Hz, 2H), 3.15 – 3.00 (m, 8H).

*Note: Hydroiodic acid is commonly stabilized with hypophosphorous acid, which can also form an ammonium salt complex and results in an inseparable mixture of halogen and phosphorus ammonium salts. To avoid this, stabilizer-free HI must be used but needs to be cleaned of degradation impurities shortly beforehand. Under minimal light, 15 mL of 57% HI was extracted with a 10:1 $CHCl_3$/tributylphosphate mixture three times (3 × 25mL) to remove the black impurities from the HI layer, producing clear 57% HI that is stored under inert atmosphere in the dark before use.

AE4T·2HX (X = Cl, I) Synthesis (see Scheme 1b in the main article):

2,2,5,5-tetramethyl-1-(2-(thiophen-2-yl)ethyl)-1,2,5-azadisilolidine (6)

12.72 g (100 mmol, 1.0 eq) thiophene-2-ethylamine was weighed out and added to a flame dried 3-neck 500 mL RBF with addition funnel under inert atmosphere, followed by 30.6 mL (22.26 g, 220 mmol, 2.2 eq) of freshly distilled, dry triethylamine added by syringe. 250 mL of dry DCM was then added to the reaction flask by cannula under inert atmosphere and the mixture was cooled to 0°C in an ice water bath while being stirred. In a separate flame-dried 250 mL RBF in a glovebox, 22.6 g (105 mmol, 1.05 eq) of 96% 1,2-bis(chlorodimethylsilyl)ethane was weighed out under inert atmosphere, removed from the glovebox, and then dissolved in 120 mL of dry DCM. The 1,2-bis(chlorodimethylsilyl)ethane solution was added to the addition funnel by cannula and slowly added to the stirring 0°C thiophene-2-ethylamine solution drop-wise. *Note: Addition of the 1,2-bis(chlorodimethylsilyl)ethane solution produces significant amounts of HCl gas. Ensure the reaction is kept under inert atmosphere and run with proper ventilation.* The reaction mixture was left to stir and react for three days. The crude RM was filtered and washed through with DCM to remove a white solid biproduct. The filtrate solution was concentrated by rotary evaporation, and then filtered a second time with hexanes to remove additional white solid biproduct. The crude product was dried overnight under high vacuum. Further purification by vacuum distillation in a 102 °C oil bath under high vacuum (0.3 torr) provided the pure desired product as a clear oil. The ^{1}H NMR spectrum of compound **6** is given in Figure S12.

Note: This protected amine stabase compound is readily deprotected by water or alcohols and is thus air and water sensitive. The product should be stored under inert atmosphere, where it will remain stable for extended lengths of time.

Yield: 19.6 g (73% yield)

^{1}H NMR (400 MHz, Chloroform-*d*) δ 7.14 – 7.10 (m, 1H), 6.94 (dd, *J* = 5.0, 3.5 Hz, 1H), 6.80 (d, *J* = 3.4 Hz, 1H), 3.13 – 3.04 (m, 2H), 2.93 – 2.83 (m, 2H), 0.72 (s, 4H), 0.07 (s, 12H).

5,5'-dibromo-2,2'-bithiophene (7)

5.02 g (30.18 mmol, 1.0 eq) of commercially available 2,2′-bithiophene was weighed out into a 100 mL RBF and then dissolved in 35 mL of dry DMF. The flask was covered with tin foil to shield the solution from light, put under an inert atmosphere, and the mixture was cooled to 0°C in an ice water bath. In a separate 100 mL tin foil covered RBF, 10.97 g (61.65 mmol, 2.05 eq) of solid NBS was dissolved in 45 mL of DMF in the dark under an inert atmosphere, while cooled to 0 °C in an ice water bath. These two flasks were stirred at 0 °C for 30 minutes. Using a 50 mL syringe, the NBS solution was added to the 0 °C flask containing 2,2′-bithiophene dropwise under minimal light while the solution was stirred vigorously. The RM was left to stir and slowly warm back to RT in the dark overnight. The next morning, the RM was poured into 200 mL of 0°C water, producing the crude product as a beige precipitate that was collected by vacuum filtration. The crude beige solid (13.1 g) was added to 300 mL of hexanes, heated until boiling, and then decanted into a 1 L Erlenmeyer flask. The crude solid was decanted a second time with an additional 300 mL of hexane. The pure product recrystallized from the combined hexanes solution and was collected by vacuum filtration, providing 7.92 g of the desired product as beige crystals. The ^{1}H NMR spectrum of compound **7** is given in Figure S13.

Yield: 7.92 g (81% yield)

^{1}H NMR (400 MHz, Chloroform-*d*) δ 6.96 (d, *J* = 3.8 Hz, 2H), 6.85 (d, *J* = 3.8 Hz, 2H).

5,5'''-bis(2-(2,2,5,5-tetramethyl-1,2,5-azadisilolidin-1-yl)ethyl)-2,2':5',2'':5'',2'''-quaterthiophene (8)

2.69 g (10 mmol, 1.0 eq) of compound **6** was added to a flame dried 250 mL RBF under inert atmosphere. The flask was purged with argon for 10 minutes, and then 50 mL of dry diethyl ether was added by cannula. The mixture was cooled to 0°C in an ice water bath, and then 4.4 mL (11 mmol, 1.1 eq) of 2.5 M *n*-BuLi in hexanes was added to the RM dropwise. After 1 hour at 0 °C, 2.84 g (11 mmol, 1.1 eq) of solid $MgBr_2 \cdot Et_2O$ under inert atmosphere was added to the 0°C RM in one portion under a flow of argon. The RM was stirred for 30 minutes at 0°C. Into a separate 250 mL flame dried RBF, 1.296 g (4 mmol, 0.4 eq) of compound **7** and 86.7 mg (0.16 mmol, 0.016 eq) of dichloro(1,3-bis(diphenylphosphino)propane)nickel ($NiCl_2$(dppp)) was weighed out and the flask was purged with argon for 10 minutes. The Grignard solution from the first flask was then added to the second flask by cannula under inert atmosphere, and the combined mixture was stirred overnight at room temperature.

The now orange crude RM was vacuum filtered and the filter solid was washed with 150 mL of diethyl ether, providing the crude product as a bright yellow solid. The crude filter solid was added to a 500 mL Erlenmeyer flask, mixed with boiling hexanes, and then decanted through filter paper into a 1 L Erlenmeyer flask. This process was repeated multiple times, using 900 mL of boiling hexanes in total. The combined hexanes fractions were concentrated by rotary evaporation to provide 1.98 g of the desired product as a bright yellow solid. The ^{1}H NMR spectrum of compound **8** is given in Figure S14.

Yield: 1.98 g (70% yield)

^{1}H NMR (600 MHz, Chloroform-*d*) δ 7.04 (d, *J* = 3.7 Hz, 2H), 7.00 (dd, *J* = 5.9, 3.7 Hz, 4H), 6.70 (d, *J* = 3.5 Hz, 2H), 3.11 – 3.06 (m, 4H), 2.87 – 2.82 (m, 4H), 0.72 (s, 8H), 0.07 (s, 24H).

5,5'''-diylbis(amino-ethyl)-[2,2':5',2'':5'',2'''-quaterthiophene] dihydrochloric acid salt AE4T·2HCl (9-Cl)

0.573 g (0.817 mmol, 1.0 eq) compound **8** was weighed out and added to a 50 mL RBF covered with tin foil to shield the reaction from light, put under inert atmosphere, and dissolved in 20 mL of chloroform. Once all of the starting material dissolved, 7 mL of 12 M hydrochloric acid was added to the stirring reaction mixture, deprotecting the amine and quickly generating the desired ammonium-halide salt as a yellow precipitate. After stirring for three hours under inert atmosphere, the ammonium-halide solid product was isolated from the crude RM by vacuum filtration. The filtered solid was washed with 10 mL of 1,4-dioxane and then 10 mL of $CHCl_3$. The product was collected and dried under high vacuum overnight, providing the pure product as a muddy yellow powder. The ^{1}H NMR spectrum of compound **9-Cl** is given in Figure S15.

Yield: 0.376 g (94% yield)

^{1}H NMR (600 MHz, DMSO-d_6) δ 7.89 (s, 6H), 7.30 (d, *J* = 2.7 Hz, 2H), 7.23 (dd, *J* = 6.3, 2.7 Hz, 4H), 7.04 – 6.94 (m, 2H), 3.09 (s, 8H).

5,5'''-diylbis(amino-ethyl)-[2,2':5',2'':5'',2'''-quaterthiophene] dihydroiodic acid salt AEQT*2HI (9-I)

0.459 g (0.49 mmol, 1.0 eq) compound **8** was weighed out and added to a 50 mL RBF covered with tin foil to shield the reaction from light, put under inert atmosphere, and dissolved in 20 mL of $CHCl_3$. Once all of the starting material dissolved, 7 mL of freshly purified, stabilizer-free* 57% hydroiodic acid was added to the stirring reaction mixture, deprotecting the amine and quickly generating the desired ammonium-halide salt as a yellow precipitate. After stirring for three hours under inert atmosphere, the ammonium-halide solid product was isolated from the crude RM by vacuum filtration. The filtered solid was washed with 30 mL of $CHCl_3$. The product was collected and dried under high vacuum overnight, providing the pure product as a solid yellow powder. The ^1H NMR spectrum of compound **9-I** is given in Figure S16.

* Note: Hydroiodic acid is commonly stabilized with hypophosphorous acid, which can also form an ammonium salt complex and results in an inseparable mixture of halogen and phosphorus ammonium salts. To avoid this, stabilizer-free HI must be used but needs to be cleaned of degradation impurities shortly beforehand. Under minimal light, 15 mL of 57% HI was extracted with a 10:1 $CHCl_3$/tributylphosphate mixture three times (3 × 25mL) to remove the black impurities from the HI layer, producing clear 57% HI that is stored under inert atmosphere in the dark before use.

Yield: 0.364 g (82% yield)

^1H NMR (600 MHz, DMSO-d_6) δ 7.78 (s, 6H), 7.11 (d, J = 3.6 Hz, 2H), 6.93 (d, J = 3.6 Hz, 2H), 3.15 – 3.00 (m, 8H).

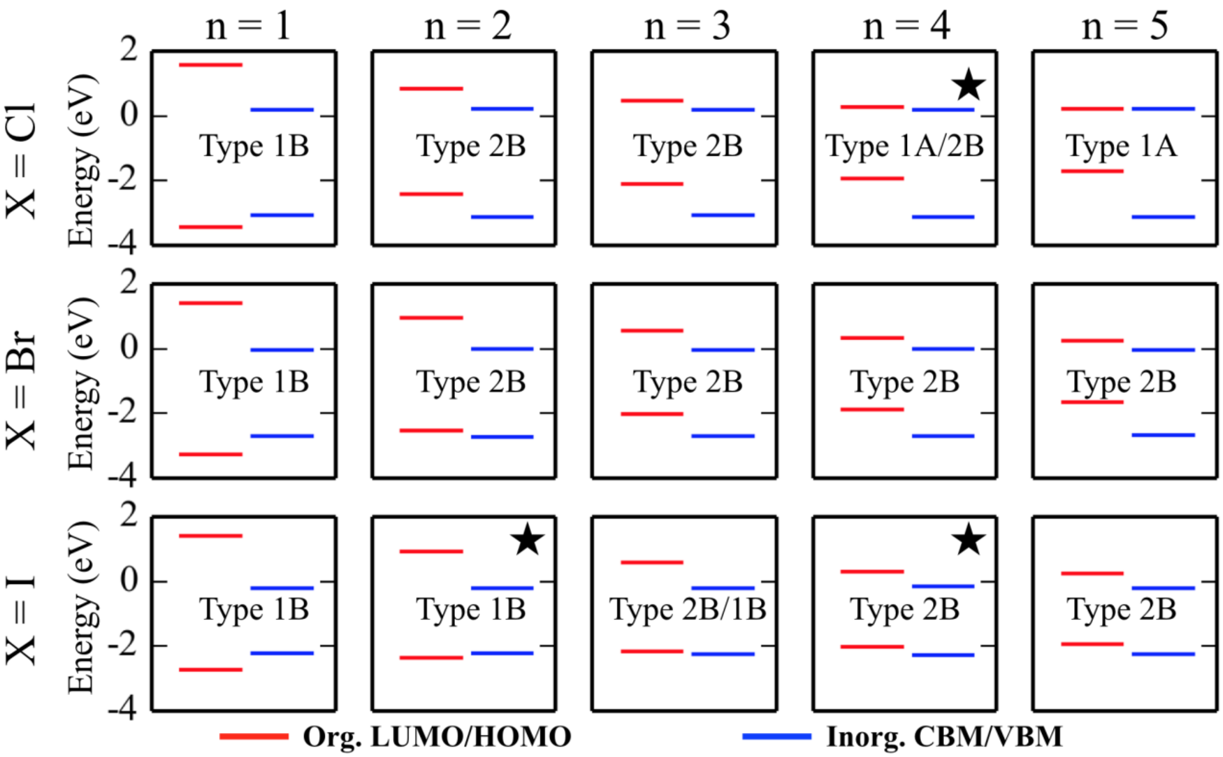

Figure S1. Band/molecular orbital alignments of the AE*n*TPbX$_4$ family (*n* = 1 - 5, X = Cl, Br, I), predicted by the hybrid HSE06[1] density functional plus spin-orbit coupling (SOC)[2] with the all-electron electronic structure code FHI-AIMS.[3-7] The energy levels of different compounds are aligned relative to the average of Pb 1s energies. The actual values of all the band/molecular orbital energies are summarized in Table S1. The band alignment type for each compound is indicated in each panel. The stars label the three compounds that are experimentally synthesized and investigated, *i.e.*, AE4TPbCl$_4$, AE2TPbI$_4$, and AE4TPbI$_4$ as representatives from Type 1A, 1B, and 2B structures, respectively. The geometry optimization is performed using the PBE exchange functional[8] plus the Tkatchenko-Scheffler (TS)[9] pairwise dispersion scheme. The FHI-AIMS' "intermediate" settings and dense k-point grids of 3 × 3 × 3 are used in the calculation of band/molecular orbital alignments. More computational details can be found in Liu *et al.* and its Supporting Information.[10]

Table S1. Band/molecular orbital energy values of the AE*n*TPbX_4 family (*n* = 1 - 5, X = Cl, Br, I) predicted by HSE06[1] + SOC[2] with the all-electron electronic structure code FHI-aims.[3-7] All values in this table are plotted in Figure S1. Computational details for obtaining these values appear in the caption of Figure S1.

Halogen	Band / Orbital Energy (eV)	Number of Thiophene Rings (n)				
		1	2	3	4	5
Cl	Org. LUMO	1.56	0.83	0.47	0.26	0.20
	Inorg. CBM	0.18	0.23	0.18	0.19	0.22
	Org. HOMO	-3.44	-2.43	-2.10	-1.93	-1.70
	Inorg. VBM	-3.08	-3.13	-3.07	-3.13	-3.13
Br	Org. LUMO	1.40	0.97	0.56	0.33	0.26
	Inorg. CBM	-0.03	0.00	-0.03	0.00	-0.03
	Org. HOMO	-3.26	-2.54	-2.01	-1.89	-1.66
	Inorg. VBM	-2.69	-2.73	-2.69	-2.70	-2.67
I	Org. LUMO	1.40	0.93	0.58	0.30	0.26
	Inorg. CBM	-0.21	-0.20	-0.20	-0.16	-0.22
	Org. HOMO	-2.73	-2.36	-2.16	-2.00	-1.94
	Inorg. VBM	-2.22	-2.22	-2.25	-2.27	-2.24

How the Configuration of the Organic Cation Impacts Lattice Parameters of AE4TPbCl$_4$. Subtle changes in the arrangements of the quaterthiophene cations in AE4TPbCl$_4$ can have significant effects on the lattice parameters of the DFT-predicted crystal structure of this material. As an example, we consider the effects of organic cation tilting in AE4TPbCl$_4$, comparing a "staggered" configuration (the crystal structure used to generate the DFT-predicted XRD pattern in this work), wherein tilting directions of the quaterthiophene are mixed within a single layer, versus the "Left_right" configuration, in which quaterthiophenes in the same layer tilt in the same direction, but in the opposite direction from those in adjacent layers (Figure S2). Our calculations show that the relaxed *a* axis increases for the latter configuration by ~3 Å (see Table S2 for a comparison of the lattice characteristics of the staggered vs. "Left_right" configurations), showing that the organic conformation can shift this value by a significant amount. This result does not imply that the "Left_right" configuration is necessarily the correct one, especially given that the total energy per atom is calculated to be higher than that of the staggered configuration by 8 meV/atom. Rather, this comparison illustrates that subtle configurational changes of the organic cation arrangement can have significant impact on the lattice parameters.

Table S2. Variation of lattice parameters, unit cell volume *V*, and total energy E_{tot} of the hybrid DFT-predicted AE4TPbCl$_4$ crystal structure for different configurations of the organic cation. The total energies, E_{tot}, of the different configuration structures are reported relative to the value of the staggered structure.

Pattern	*a* (Å)	*b* (Å)	c (Å)	α	β	γ	*V* (Å^3)	E_{tot} (meV/atom)
Staggered	40.85	11.29	10.95	90.0°	91.8°	90.0°	5049	0
Left_right	44.12	11.49	10.56	97.6°	93.0°	89.9°	5297	8

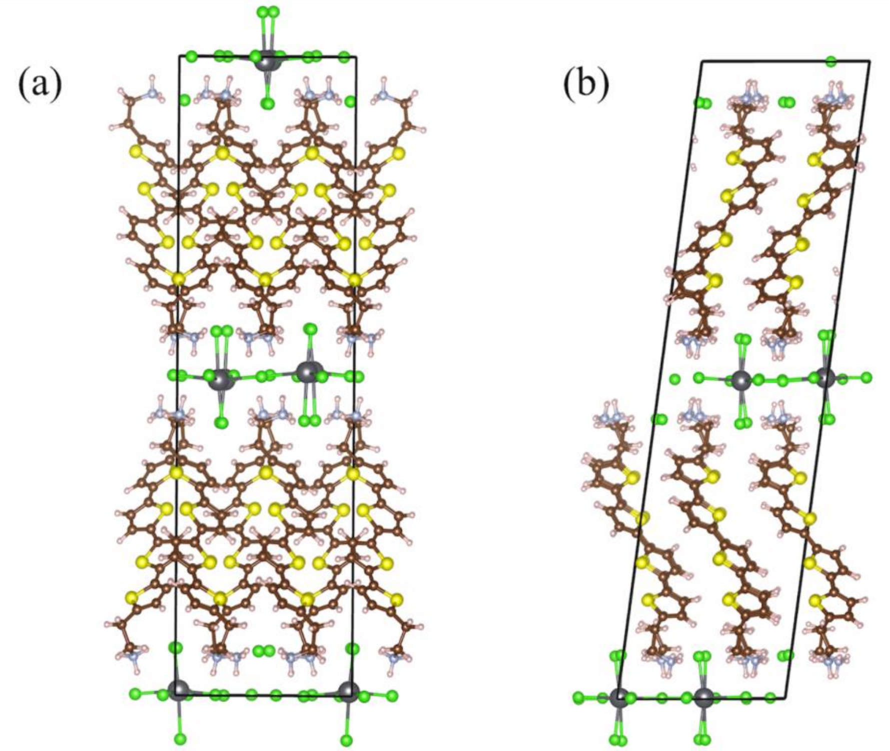

Figure S2. Illustrations of the "staggered" (a) and "left_right" (b) configurations of the organic in hybrid DFT calculations of the AE4TPbCl4 crystal structure.

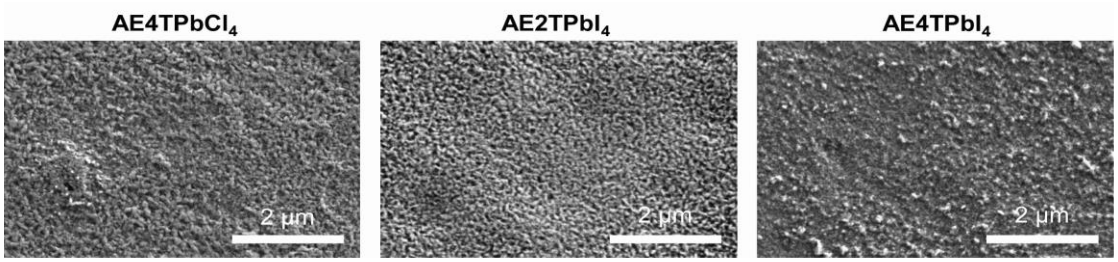

Figure S3. SEM images of RIR-MAPLE-deposited oligothiophene perovskite films on glass/ITO substrates.

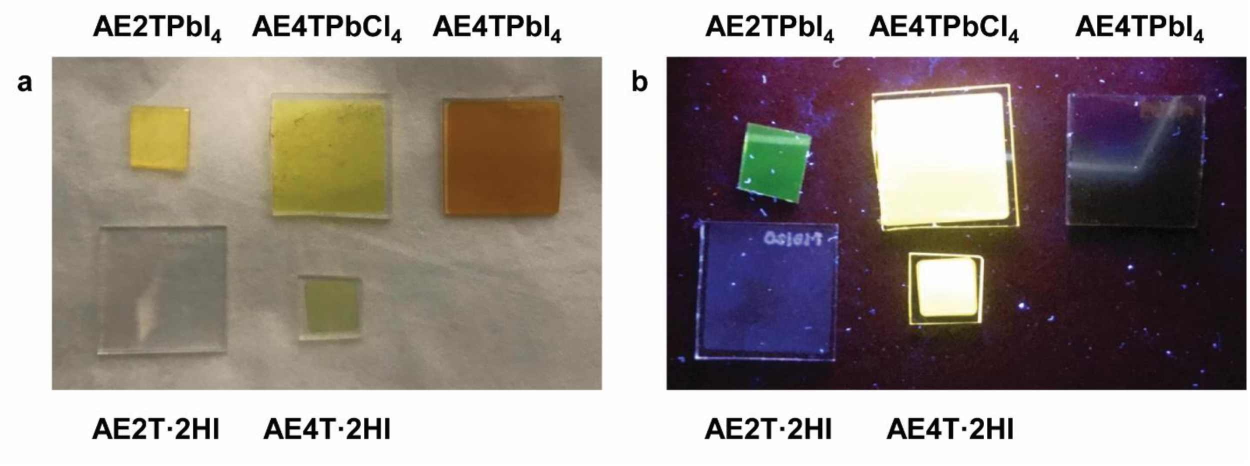

Figure S4. Photographs of RIR-MAPLE-deposited perovskite and oligothiophene salt films under ambient indoor (a) and 365 nm ultraviolet light (b), displaying the characteristic luminescence of each material (except for AE4TPbI$_4$, which does not fluoresce strongly, as discussed in the main text). The larger films are approximately 2 cm by 2 cm; the small ones are ~1 cm^2.

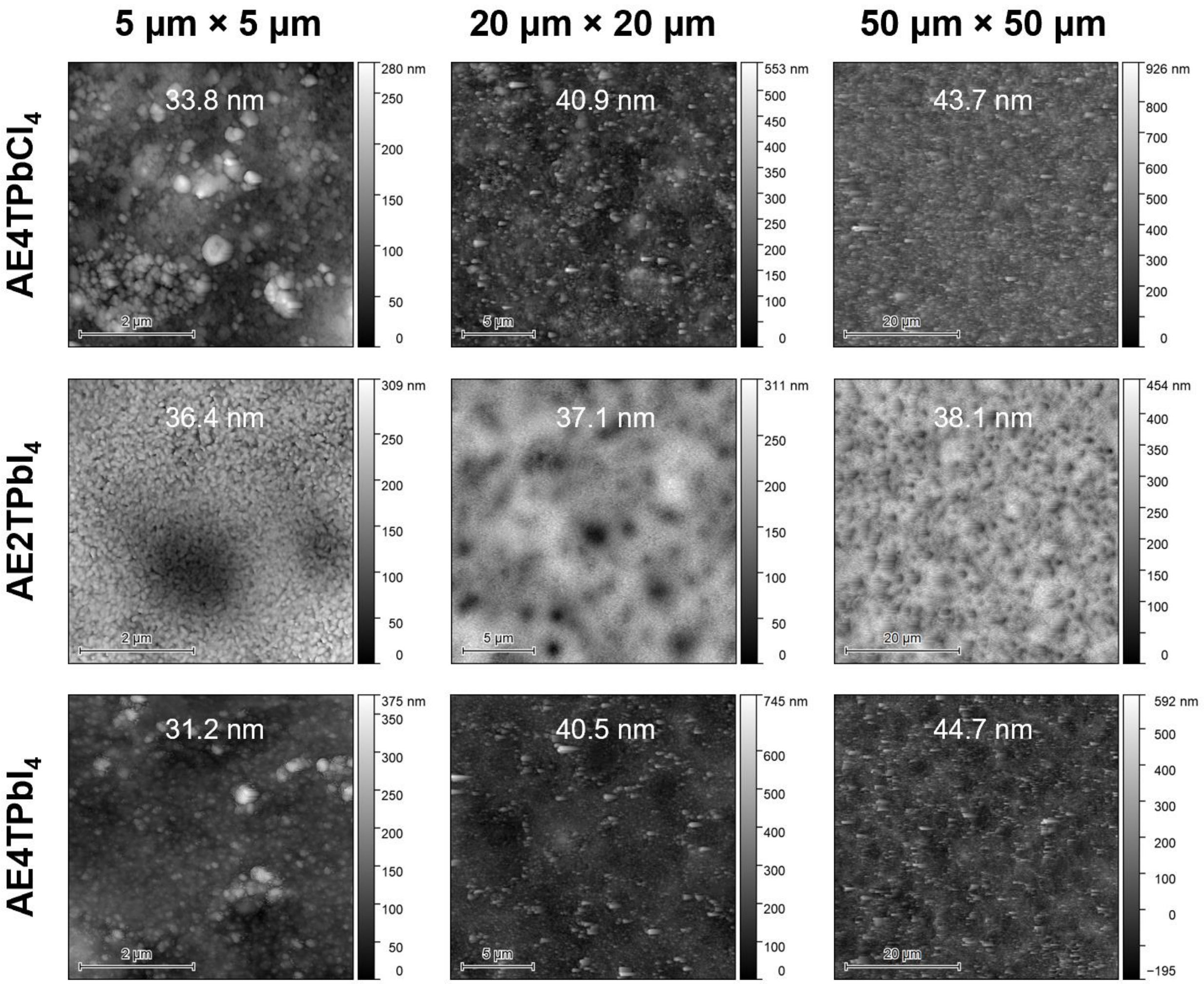

Figure S5. AFM images of RIR-MAPLE-deposited perovskite films at different scales, showing similar morphology and RMS roughness (displayed near the top of each image) to that of previously reported[11] $CH_3NH_3PbI_3$ films deposited by the same technique.

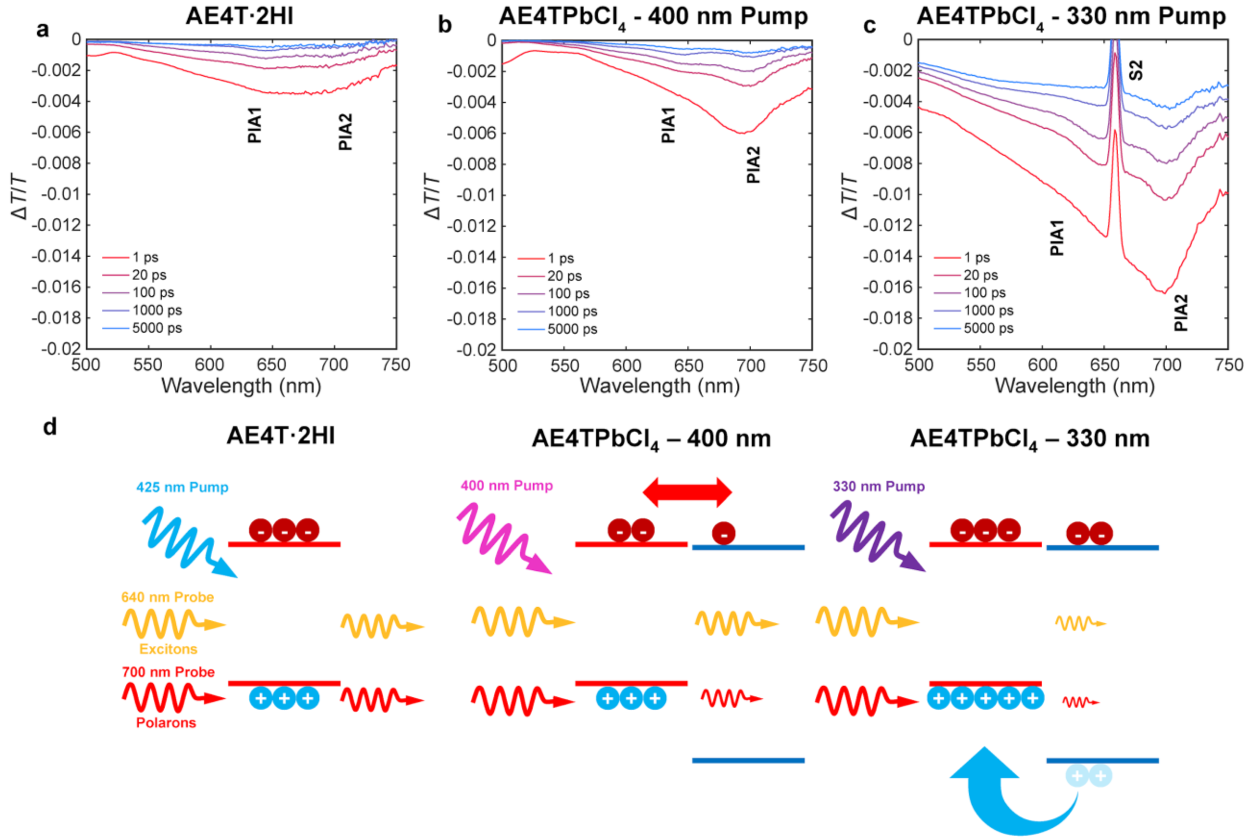

Figure S6. TAS spectra for various time delays of, AE4T·2HI taken with pump wavelength 425 nm (a), AE4TPbCl$_4$ taken with pump wavelength 400 nm (b), and AE4TPbCl$_4$ taken with pump wavelength 330 nm (c); band diagram/carrier population schematics for these scenarios (d). PIA1, PIA2, and S2 denote features associated with AE4T excitons, AE4T hole polarons, and scattered pump light, as noted in the main text.

The spectra shown in Figure S6 are employed to help distinguish the exciton (PIA1) and polaron (PIA2) features in the quaterthiophene-containing compounds. In organic compounds it is well known that, while optical excitations primarily create excitons, there is always some polaron generation even if there is a strong exciton binding energy. The polarons and excitons both exhibit PIA features below the band gap. In blended materials, the polaron yield increases due to interface charge generation. In Figure S6a, corresponding to a film of the AE4T·2HI salt as a proxy for the neat organic, PIA1 and PIA2 are two broad features located at 640 nm and 700 nm. Due to the broadness of the spectral lines and their significant overlap, they can be more easily resolved at later delays. In AE4T·2HI, these two features exhibit very similar dynamics. The same features are evident in the spectra of AE4TPbCl$_4$ when excited with a 400 nm pump beam, which should only excite excitons in the organic part. However, in this case the strength of PIA2 is enhanced relative to PIA1. Because the organic LUMO is resonant with the inorganic CBM, electrons are likely to diffuse into the empty CBM from the relatively populated LUMO when excited by the pump beam. The holes/hole polarons in the organic part, by contrast, face a significant energy barrier to intercomponent transfer and therefore remain there. As a result, PIA2 can be assigned to the polaron feature (dependent only on the hole population in the organic), which is heightened relative to the exciton feature PIA1 (dependent on the joint density of electron and holes in the organic) in this scenario. This assignment is further supported in TAS data presented in Figure S6c. Here, when AE4TPbCl$_4$ is excited with a 330 nm pump of sufficient energy to generate excitons in both moieties, the overall intensity of both PIA1 and PIA2 is further increased. In this case, both excitations from organic and inorganic part contribute to the polaron yield.

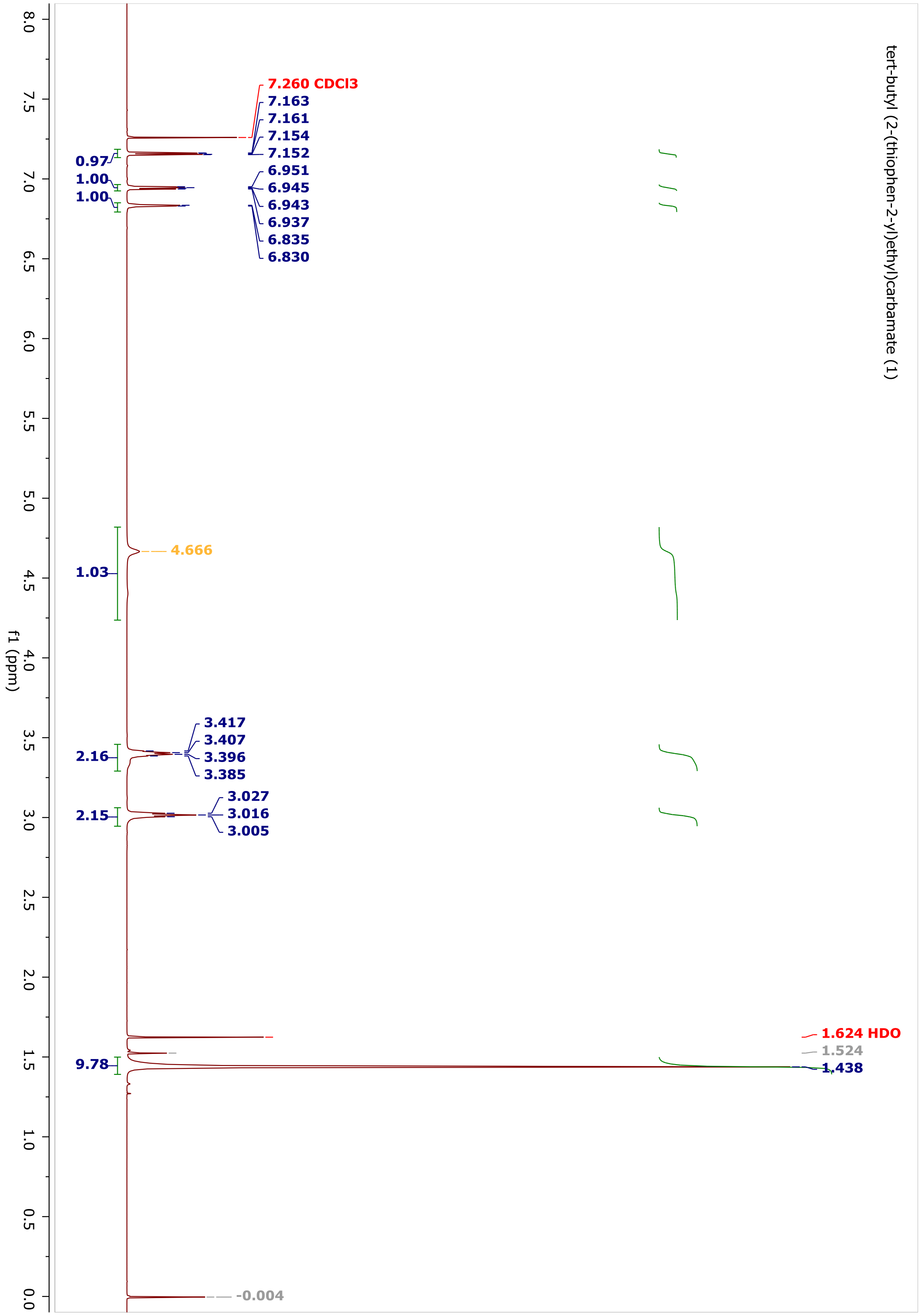

Figure S7. ^{1}H NMR spectrum of compound **1** (tert-butyl(2-(thiophen-2-yl)ethyl)carbamate) used in the synthesis of bithiophene lead halides (see Scheme 1 in the main text).

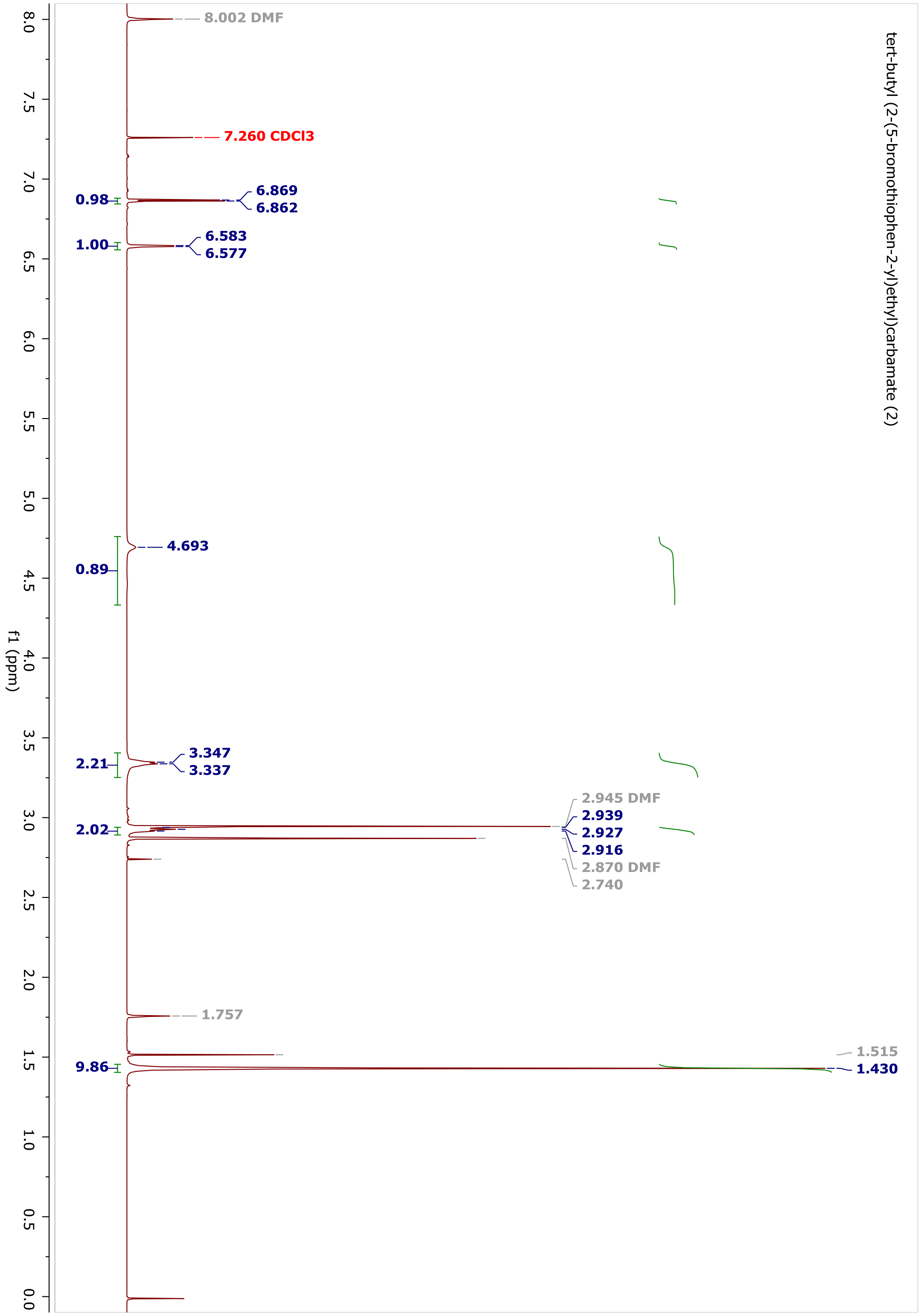

Figure S8. ^{1}H NMR spectrum of compound **2** (tert-butyl(2-(5-bromothiophen-2-yl)ethyl)carbamate) used in the synthesis of bithiophene lead halides (see Scheme 1 in the main text).

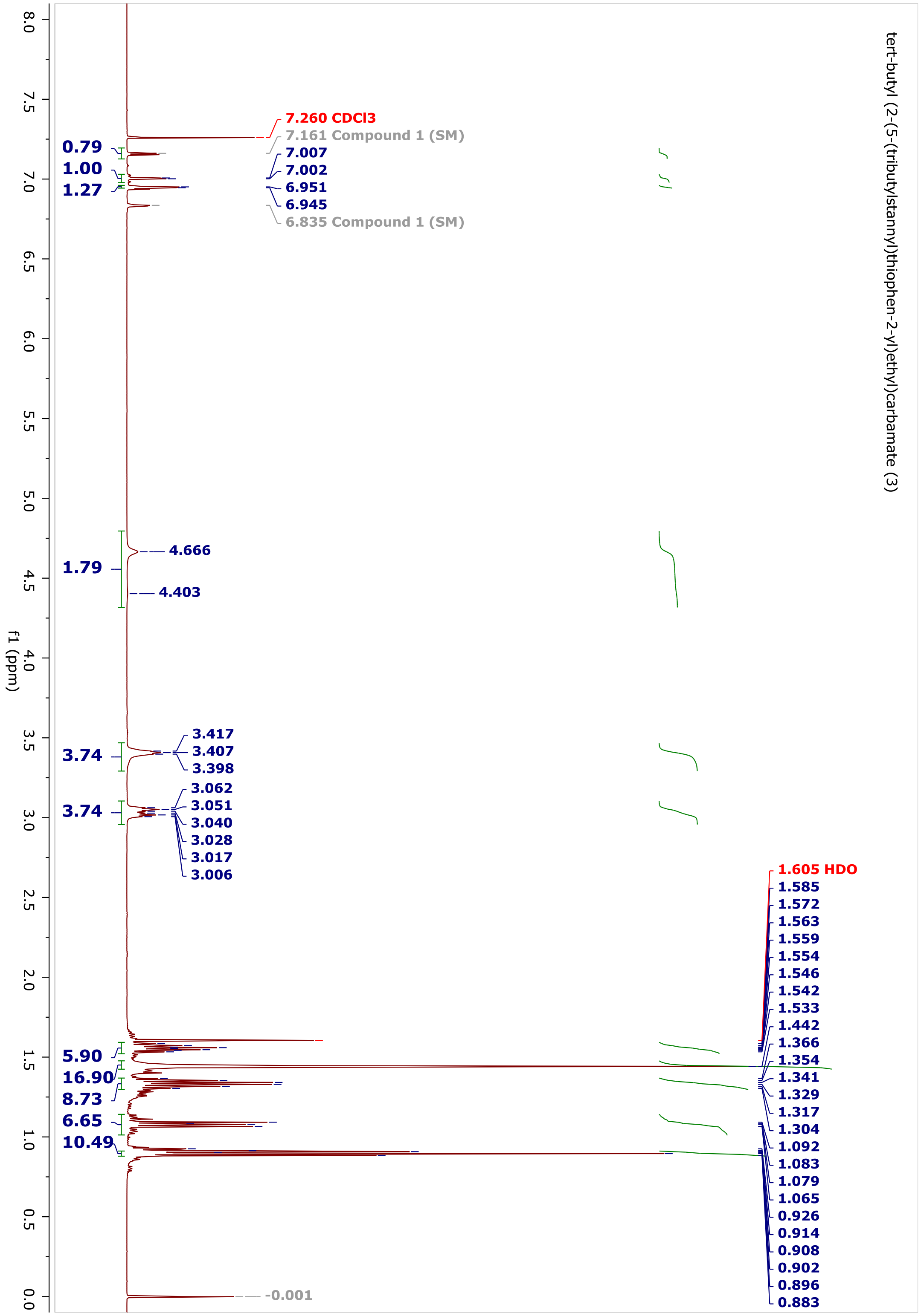

Figure S9. ^{1}H NMR spectrum of the mixture of compounds **1** and **3** (tert-butyl (2-(5-(tributylstannyl)thiophen-2-yl)ethyl)carbamate) used in the synthesis of bithiophene lead halides (see Scheme 1 in the main text).

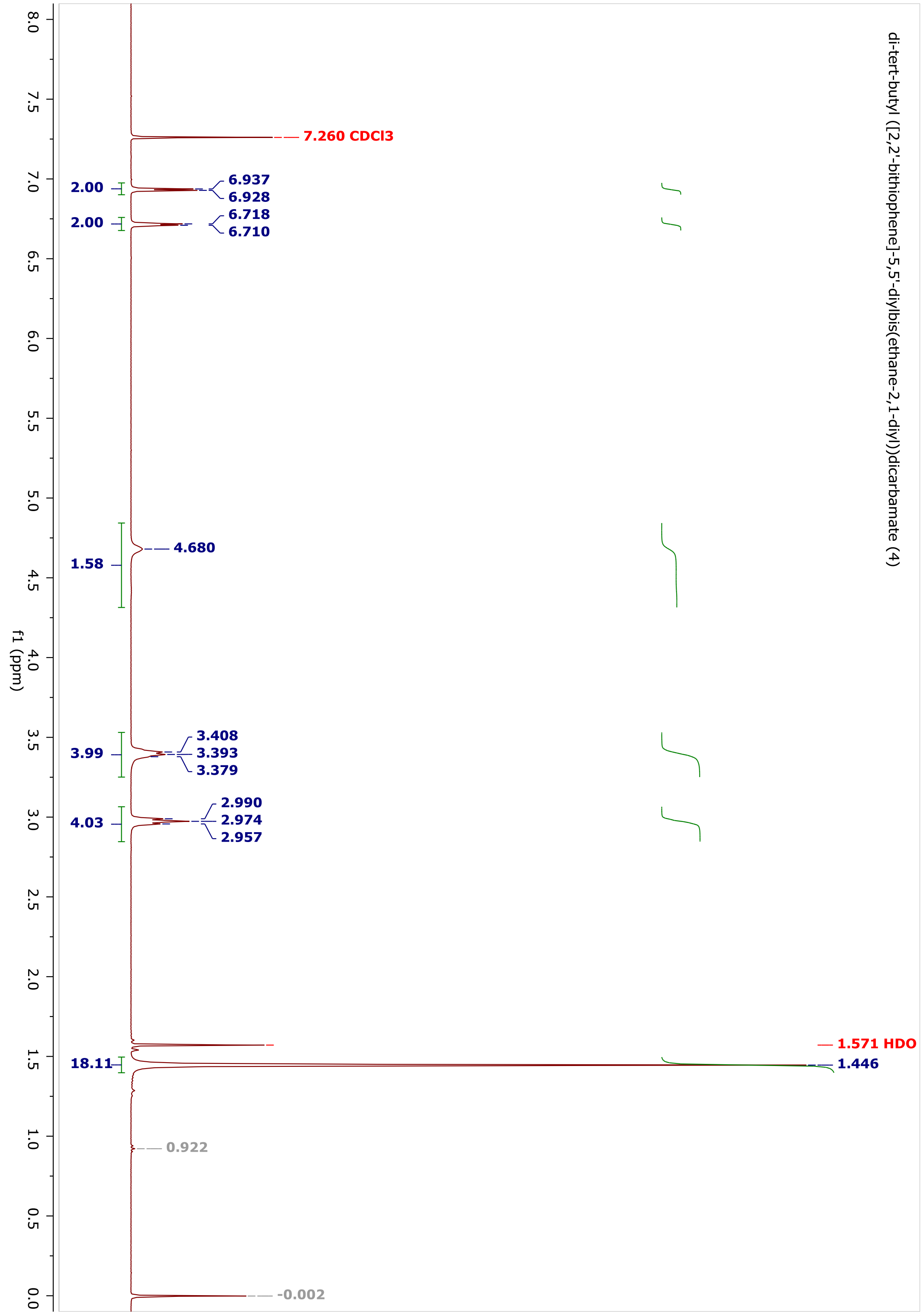

Figure S10. ^{1}H NMR spectrum of compound **4** (di-tert-butyl ([2,2'-bithiophene]-5,5'-diylbis(ethane-2,1-diyl))dicarbamate) used in the synthesis of bithiophene lead halides (see Scheme 1 in the main text).

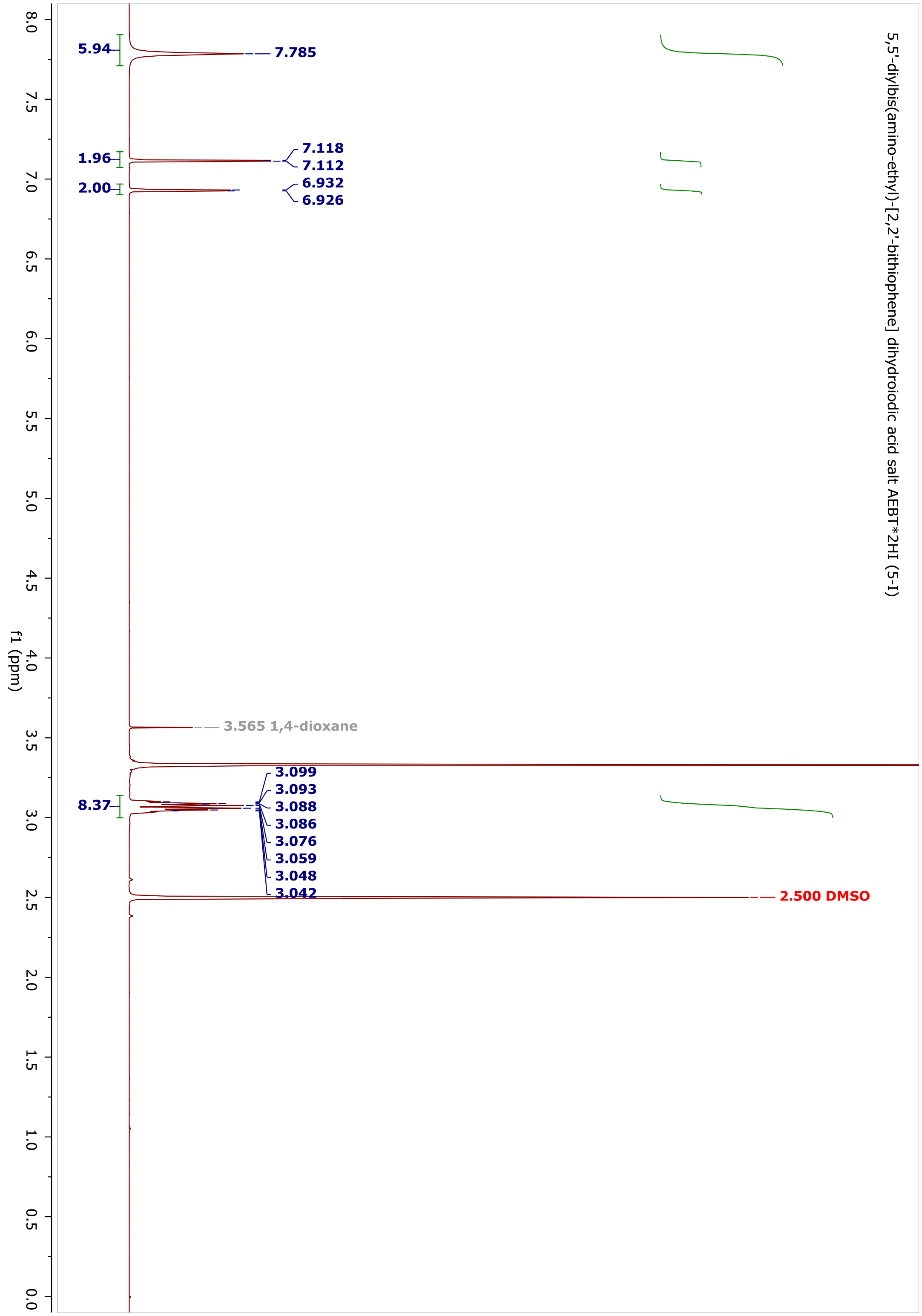

Figure S11. ^{1}H NMR spectrum of compound **5-I** (5,5'-diylbis(amino-ethyl)-[2,2'-bithiophene] dihydroiodic acid salt/AE2T·2HI) (see Scheme 1 in the main text).

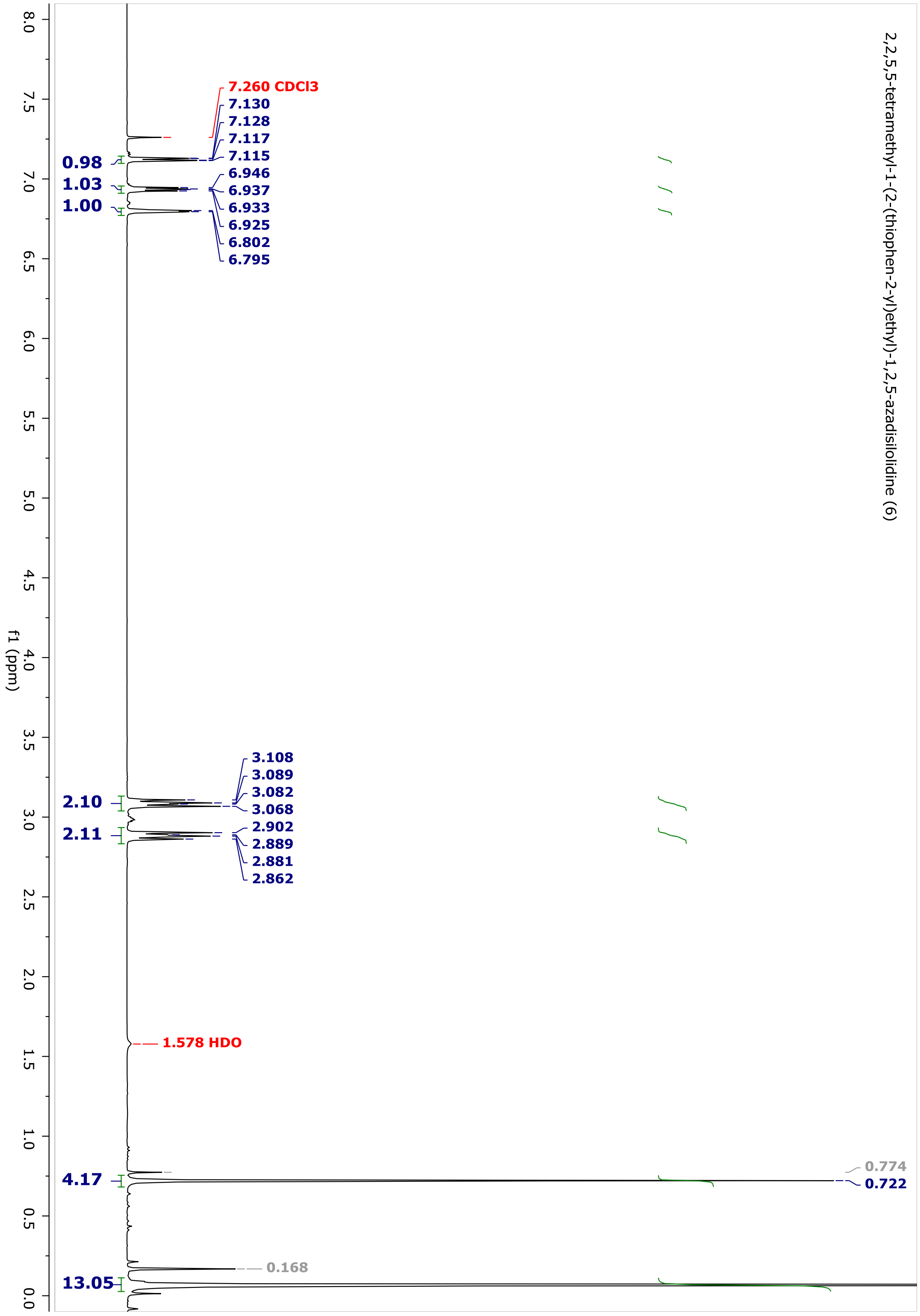

Figure S12. ^{1}H NMR spectrum of compound **6** (2,2,5,5-tetramethyl-1-(2-(thiophen-2-yl)ethyl)-1,2,5-azadisilolidine) (see Scheme 1 in the main text).

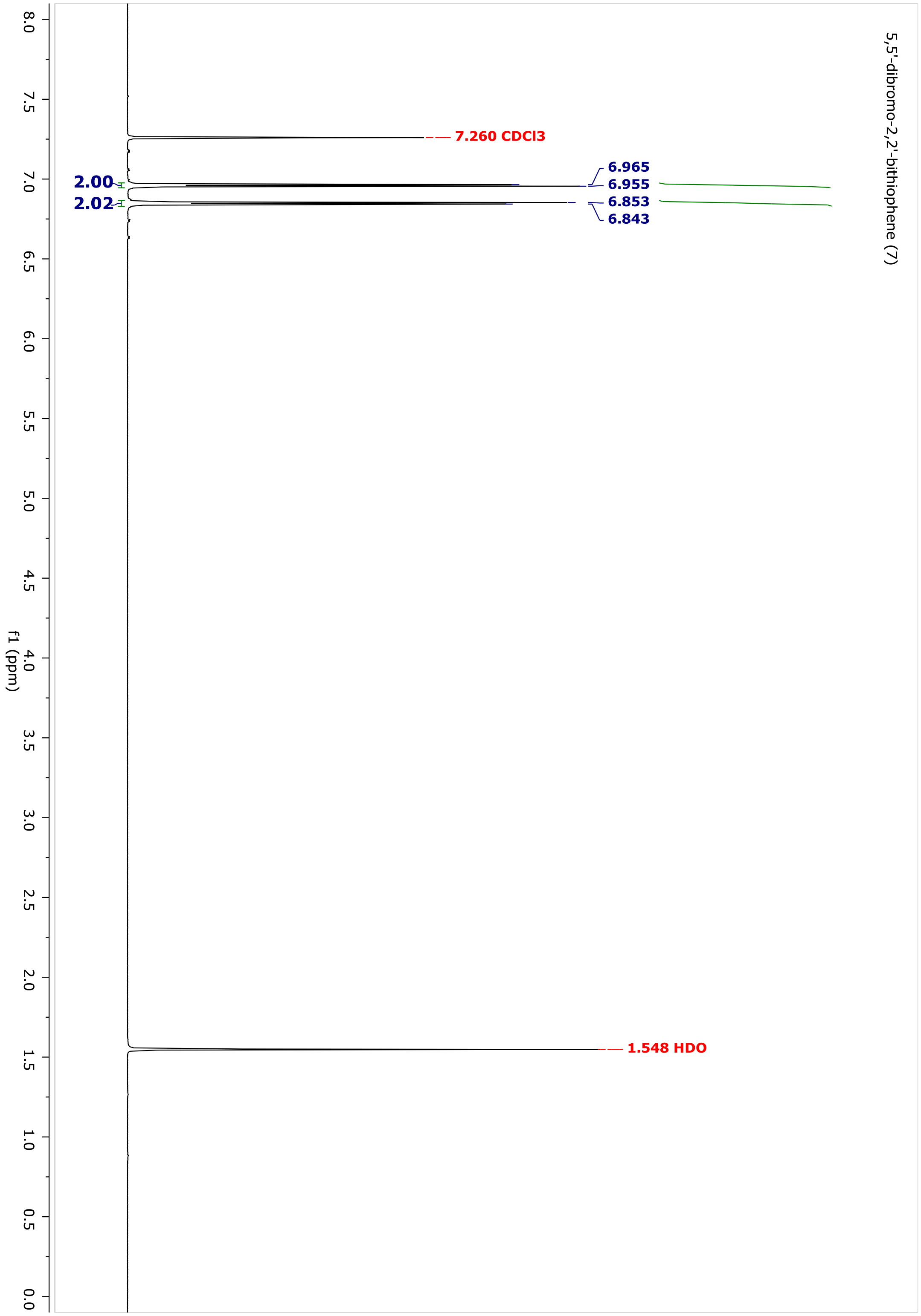

Figure S13. ^1H NMR spectrum of compound **7** (5,5'-dibromo-2,2'-bithiophene) (see Scheme 1 in the main text).

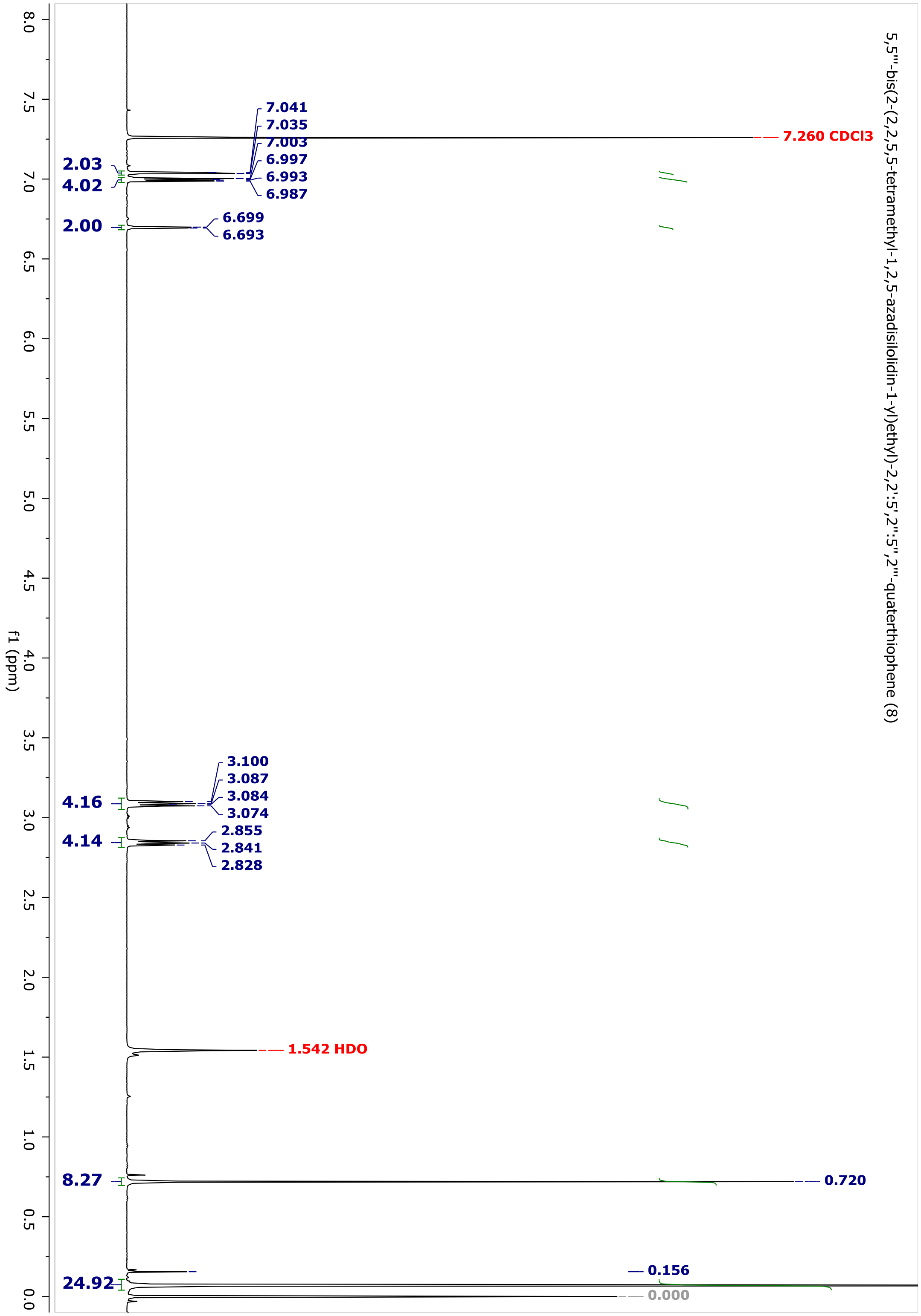

Figure S14. ^{1}H NMR spectrum of compound **8** (5,5'''-bis(2-(2,2,5,5-tetramethyl-1,2,5-azadisilolidin-1-yl)ethyl)-2,2':5',2'':5'',2'''-quaterthiophene) (see Scheme 1 in the main text).

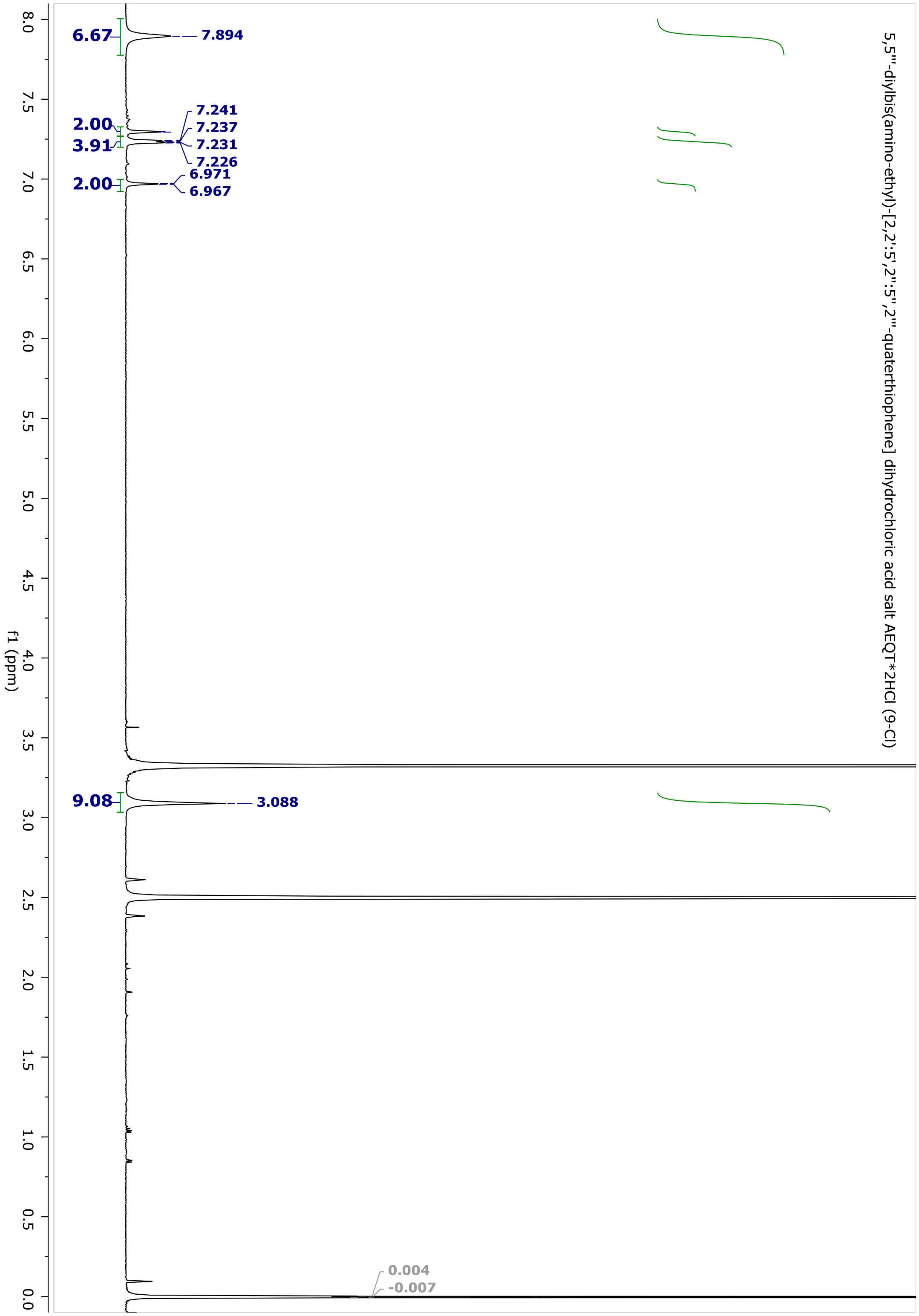

Figure S15. ^{1}H NMR spectrum of compound **9-Cl** (5,5'''-diylbis(amino-ethyl)-[2,2':5',2'':5'',2'''-quaterthiophene] dihydrochloric acid salt/AE4T·2HCl) (see Scheme 1 in the main text).

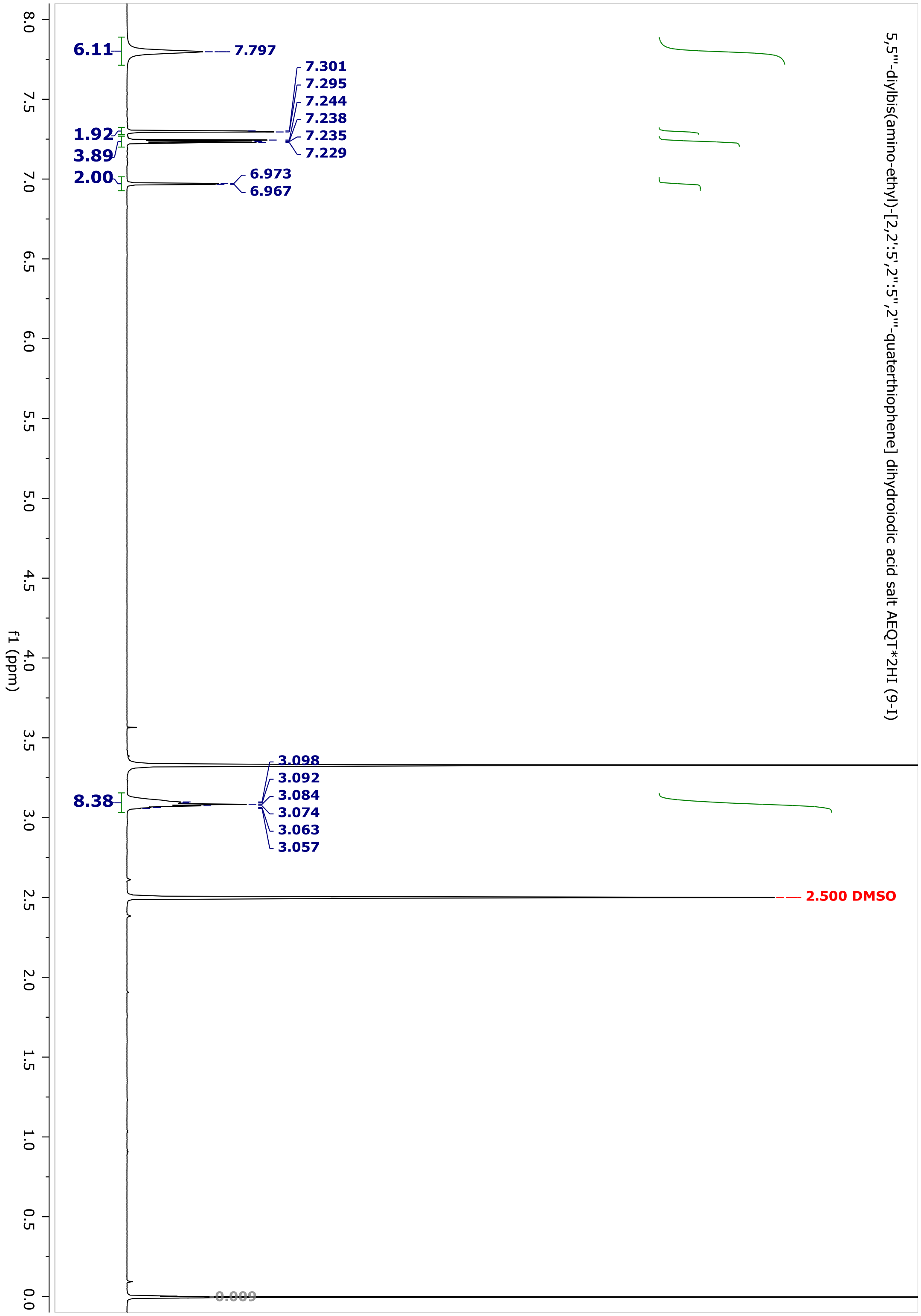

Figure S16. ^{1}H NMR spectrum of compound **9-I** (5,5'''-diylbis(amino-ethyl)-[2,2':5',2'':5'',2'''-quaterthiophene] dihydroiodic acid salt/AE4T·2HI) (see Scheme 1 in the main text).

References.

1. J. Heyd, G. E. Scuseria and M. Ernzerhof, *J. Chem. Phys.*, 2006, **124**, 219906.
2. W. Huhn and V. Blum, *Phys. Rev. Mater.*, 2017, **1**, 033803.
3. V. Blum, R. Gehrke, F. Hanke, P. Havu, V. Havu, X. Ren, K. Reuter and M. Scheffler, *Comput. Phys. Commun.*, 2009, **180**, 2175-2196.
4. V. Havu, V. Blum, P. Havu and M. Scheffler, *J. Comput. Phys.*, 2009, **228**, 8367-8379.
5. A. C. Ihrig, J. Wieferink, I. Y. Zhang, M. Ropo, X. Ren, P. Rinke, M. Scheffler and V. Blum, *New J. Phys.*, 2015, **17**, 093020.
6. S. V. Levchenko, X. Ren, J. Wieferink, R. Johanni, P. Rinke, V. Blum and M. Scheffler, *Comput. Phys. Commun.*, 2015, **192**, 60-69.
7. X. Ren, P. Rinke, V. Blum, J. Wieferink, A. Tkatchenko, A. Sanfilippo, K. Reuter and M. Scheffler, *New J. Phys.*, 2012, **14**, 053020.
8. J. P. Perdew, K. Burke and M. Ernzerhof, *Phys. Rev. Lett.*, 1996, **77**, 3865-3868.
9. A. Tkatchenko and M. Scheffler, *Phys. Rev. Lett.*, 2009, **102**, 073005.
10. C. Liu, W. Huhn, K. Z. Du, A. Vazquez-Mayagoitia, D. Dirkes, W. You, Y. Kanai, D. B. Mitzi and V. Blum, *Phys. Rev. Lett.*, 2018, **121**, 146401.
11. W. A. Dunlap-Shohl, E. T. Barraza, A. Barrette, K. Gundogdu, A. D. Stiff-Roberts and D. B. Mitzi, *ACS Energy Lett.*, 2018, **3**, 270-275.